Macromolecules

Article

pubs.acs.org/Macromolecules

Surface-Induced Nanostructure and Water Transport of Thin Proton-Conducting Polymer Films

Sangcheol Kim,*[,†] Joseph A. Dura,[‡] Kirt A. Page,*[,†] Brandon W. Rowe,[†] Kevin G. Yager,[§] Hae-Jeong Lee,[†] and Christopher L. Soles[†]

[†]Materials Science and Engineering Division, National Institute of Standards and Technology, Gaithersburg, Maryland 20899, United States

[‡]Center for Neutron Research, National Institute of Standards and Technology, Gaithersburg, Maryland 20899, United States

[§]Center for Functional Nanomaterials, Brookhaven National Laboratory, Upton, New York 11973, United States

Supporting Information

ABSTRACT: We quantify the interfacial nanostructure and corresponding water transport kinetics in thin films of Nafion which are known to show nonbulk like transport properties using neutron reflectivity (NR) and quartz-crystal microbalance (QCM) measurements integrated with in-situ, controlled relative humidity environments. Rigorous fitting of the NR data under humidified conditions reveals that a hydrophilic organosilicate substrate induces an interfacial layering of the water transport domains parallel to the substrate whereas the hydrophobic organosilicate analogue does not trigger this interfacial ordering. The interfacial layering on the hydrophilic substrate is accompanied by an excess in the total mass of water absorption as verified by QCM measurements. The excess water in the thin Nafion films is quantitatively consistent with the segregation amounts and length scales quantified by NR. However, we do not observe strong differences in the water transport kinetics in thin Nafion films where the volume fraction of the materials with the water transport oriented parallel substrate, orthogonal to the primary direction of transport, is on the order of ≈7 vol %; to a first approximation the majority of the transport kinetics are similar on the hydrophilic (oriented) and hydrophobic (disordered) surfaces.

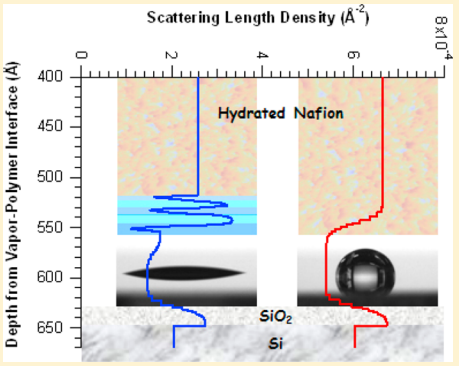

INTRODUCTION

Despite decades of fuel cell research and development, Nafion[1] remains the most prominent and widely studied proton exchange fuel cell (PEFC) membrane material, owing to its thermal stability, chemical stability, and superior performance as a proton transport media. PEFCs must provide high mobility for ion transport pathways while operating under harsh conditions that include low pH, elevated temperatures, electrochemical potentials across large interfacial areas, and cyclic exposures to hydration, temperature, and swelling stresses. Despite significant efforts to reduce the cost and/or improve the performance of Nafion, suitable replacements have yet to be realized; Nafion remains the PEFC membrane material of choice for the fuel cell community.

While the importance of Nafion as the industry standard PEFC membrane is widely recognized, its performance under interfacial or thickness-confined conditions has not been fully appreciated. In addition to the PEFC membrane itself, Nafion is a critical component in the catalyst layer of the membrane electrode assembly (MEA) as an active binder to interface the ion transport media, the gas transport channels, the electrochemical catalyst particles, and the electrically conductive media that interface the ion transport media with the electrodes.[2,3] To balance ion, electron, and gas transport in the MEA, the resulting structure must be highly porous and interconnected in a way that maximizes all the relevant transport pathways. The typical solution is an electrode composite layer where Nafion is used as a binder to hold together electrically conductive carbon nanoparticles with catalytically active Pt particles in a highly porous and interconnected network.[4−6] In this MEA structure, the thickness of the Nafion domains is typically on the order of tens of nanometers or less. It is known that many fundamental properties of polymeric materials show significant deviations from their bulk values when they are confined to films or interfaces with dimensions approaching tens of nanometers. While the water and proton transport properties of thick Nafion membranes under humidified conditions are well-understood, very little is quantitatively known about the transport behavior in the interfacial and confined regions that make up the MEA. These interfacial effects can become significant when one considers the level of porosity in the MEA and the amount of interfacial or thickness-confined Nafion present.

Received: April 10, 2013
Revised: June 14, 2013
Published: July 5, 2013

Simulation and modeling are widely used in fuel cells to optimize device performance. In a PEFC assembly, hydrogen catalytically oxidizes to hydronium on one side of the membrane and then reacts with oxygen on the other side to extract electrical current. As water is a byproduct of this reaction, it is important to rapidly remove the water vapor from the cathode to drive the reaction forward. An accumulation of liquid water near the cathode will slow down the reaction kinetics. Simulation and modeling of the entire fuel cell at the systems level can be important tools to optimize the complicated transport models that take into account the flow of hydronium ions across the humidified bulk membrane, through the active Nafion binder in the MEA to the catalytic particles, as well as the flow of hydrogen, oxygen, and water vapor either into or out of the electrode structures. While this is a complicated transport problem, most of the parameters have been validated to the point where simulation and modeling are now powerful tools for optimizing performance and water management.[7,8] However, these models still require the addition of an empirical interfacial impedance term to account for the water and proton transport in the interfacial Nafion domains of the MEA. Recently, the behavior at the water vapor−polymer interface has started to receive attention,[9−15] but there are only a few reports addressing the properties of Nafion at various interfaces and surfaces[16−20] because the techniques to probe near the buried interfaces are limited. A detailed understanding of the transport mechanisms in these interfacial and confined Nafion domains is critical for improving the systems engineering and performance of PEFCs.

Dura and co-workers initially reported an interfacial layering, which could persist up to ≈7 nm from the interface, of the water transport domains adjacent to the native and thermal oxides on a silicon substrate, but it did not occur on gold or platinum coated substrates.[21,22] More recently, Eastman and co-workers reported a significant suppression of the transport kinetics and uptake of water into Nafion on the time scales that were investigated when the film thickness dropped below 60 nm.[23] It is reasonable to question if these deviations in the transport kinetics become evident at a film thickness where the previously reported effect of interfacial layering would start to comprise a significant fraction of the film thickness. In this report, we explore this possibility with well-defined planar films of Nafion on smooth substrates as a model platform to quantify both the structure and transport properties of Nafion confined at thicknesses that are relevant to the MEA.

The focus of the current study is to control the interfacial layering of the water transport domains and determine if the presence of this interfacial layering leads to changes in the transport kinetics. To do this, flat substrates were prepared using a spin-on organosilicate glass (OSG), which can be readily spin-cast onto either a thick silicon wafer for the neutron reflectivity (NR) measurements or the active electrodes of quartz-crystal microbalance (QCM) substrates. This OSG, normally very hydrophobic, can be rendered hydrophilic by either chemical or plasma treatment,[24,25] providing a common platform to tune the surface energy for both NR and QCM measurements. Both the NR and QCM measurements were equipped with a controlled relative humidity chamber to investigate the structure and water transport kinetics of thin Nafion films cast on OSG-modified substrates.

EXPERIMENTAL SECTION

A cubic silsesquioxane monomer, designed to maximize the number of closed-cage structures in the final cross-linked network, octa(triethoxysilylethyl)(octadimethylsiloxy)octasilsesquioxane (OTSE), was obtained from Mayaterials[1] and used without further purification to create the nanoporous substrate. First, the OTSE monomer was hydrolyzed in an acidic environment with copious amounts of water to maximize the silanol content. The hydrolyzed monomer was precipitated out of solution, dried, dissolved in propylene glycol monomethyl ether acetate (PGMEA), and then spin-cast onto the substrates (silicon wafer or QCM substrate) at 209 rad/s.[25] The silicon substrates were cleaned prior to spin coating in an ultraviolet-ozone cleaner (Jelight UVO-cleaner, model 42) for 20 min to remove organic contamination and improve adhesion. The as-cast films were vitrified into a cross-linked organosilicate glass (OSG) at 450 °C for 2 h under a nitrogen atmosphere. The as-vitrified OSG films were hydrophobic with a static water contact angle (Kruss G2) of 91 ± 2°. Exposure to UVO radiation readily renders these OSG surfaces hydrophilic. As the exposure time increased, the water contact angle decreased and the surface became completely wetted after 8 min. X-ray photoelectron spectroscopy (XPS, Kratos AXIS Ultra DLD spectrometer) measurements revealed that the C−O content was approximately 8% for the hydrophobic as-prepared OSG surface and then increased to approximately 28% after 10 min of UVO exposure. This is accompanied by the appearance of approximately 10% carboxyl (O−C═O) functionality. The nature of these chemical modifications of the UVO-treated OSG is consistent with the change from a hydrophobic to hydrophilic surface. Tapping mode atomic force microscopy measurements using a Dimension 3100 scanning force microscope (SFM, Digital Instruments, Inc.) confirm that the UVO treatment did not affect the surface roughness. For the remainder of the article, we will focus on comparing the response of thin Nafion films on the as-prepared hydrophobic OSG surface to the hydrophilic OSG that has been UVO treated for 10 min. Nafion solutions (1100 equiv molecular mass, dissolved 20 mass % in a mixture of lower aliphatic alcohols and water, containing 34 mass % water, Sigma-Aldrich Co.) were diluted in anhydrous ethanol at a ratio of 1:16 by volume. After thorough mixing, the viscous Nafion solution was dispensed on the OSG-modified substrates and immediately spin-cast at 367 rad/s for 1 min. The films were then annealed in a vacuum oven for 1 h at 60 °C, below the α-relaxation temperature of Nafion.[21]

X-ray porosimetry (XRP) was employed to determine the porosity and density depth profiles in the OSG layers on Si substrate.[24,26,27] Specular X-ray reflectivity (SXR) data of the OSG films were collected both under vacuum and in the presence of saturated toluene vapor. The porosity is then defined as the volume ratio of the pores filled with condensed toluene to the volume of the film. The as-prepared OSG film exhibited a slightly densified skin layer approximately 2.8 nm thick on a bottom layer approximately 5.4 nm thick, with porosities corresponding 5.0 and 7.8 vol %, respectively. More than two layers did not improve the quality of fitting significantly. The 10 min UVO exposure increased the density of both of these OSG layers, decreasing the porosity to 3.5% in the top layer and 4.8% in the bottom layer. These porosities and changes in the porosities upon UVO exposure are in-line with similar measurements on comparable organosilicate films.[22]

Neutron reflectometry (NR) data were taken at the Advanced Neutron Diffractometer/Reflectometer (AND/R)[28] at the NIST Center for Neutron Research according to procedures described previously.[21] The specularly reflected intensity was measured as a function of incident angle between the range of $0° < 2\theta < 13°$, for a maximum wave vector perpendicular to the substrate of $Q_z = 0.4147$ Å^{-1}. After the background scattering was subtracted, the specularly reflected intensity was normalized by a slit scan to yield the reflectivity as a function of Q_z. The data reduction and analysis of the NR data were performed using the reflpak software,[29] and the depth profile of the neutron scattering length density (SLD) through the film thickness was determined from the least-squares fit. Because of the strong SLD contrast between water (proton rich) and the Nafion (proton

dx.doi.org/10.1021/ma400750f | Macromolecules 2013, 46, 5630−5637

deficient) film, it is straightforward to use a rule of mixtures to convert the experimental SLD values into water concentration profile as a function of thickness through the film. The relative humidity or partial pressure of water inside the neutron reflectivity sample chamber was controlled by simultaneously regulating sample temperature and the dew point of H_2O, as described elsewhere.[21] Thin Nafion films were prepared according to the procedures described above on thick Si wafers (ca. 5 mm thick to ensure planarity) treated with both the hydrophilic and hydrophobic OSG surfaces. The responses of these substrates, both before and after applying the thin Nafion films, were measured under both 0% and 90% RH at a temperature of 33 °C.

In-situ grazing-incidence small-angle X-ray scattering (GISAXS) measurements were performed at the X9 undulator-based beamline at the National Synchrotron Light Source to characterize the structure in the thin Nafion films. An incident X-ray beam of energy 13.5 keV (wavelength = 0.0918 nm) was collimated using a two-slit system and focused to a beam 100 μm wide by 60 μm tall using a Kirkpatrick–Biaz mirror system. After equilibrating the samples inside a small, humidity-controlled chamber equipped with Kapton windows, the scattering was measured over a range of incidence angles, from below to above the film–air critical angle. Two-dimensional scattering images were recorded using a charge-coupled device (CCD) detector and converted to q-space using silver behenate powder as a standard.

The kinetics of water absorption and desorption into and out of the Nafion films on both the hydrophobic and hydrophilic OSG surfaces were measured using a quartz crystal microbalance (QCM, Q-Sense E1 system) in a humidity-controlled cell. Pt-coated AT-cut quartz crystals (5 MHz, 14 mm diameter) obtained from Q-Sense were modified with the OSG surface treatment described above to obtain either the hydrophobic or hydrophilic surfaces. It is critical that both hydrophobic and hydrophilic surface modifications occur in a single material and can be readily applied to a range of substrates. Rudimentary water contact angle measurements confirmed that these substrates had the same surface energies as the NR substrates. We did not perform a detailed comparison of the Nafion interfacial structure on these QCM substrates directly (they are too small for NR and XR measurements). Two external mass flow controllers were connected in parallel to the QCM sample chamber and programmed to deliver either dry air (0% RH), humidified air (100% RH), or any mixture of the two sources at a constant total flow rate of 500 ± 5 mL/min. Using this system, we can seamlessly switch between 0% and 70% RH conditions to monitor the absorption/desorption kinetics of water in the thin Nafion films on different substrates. The advantage of the QCM technique is that it offers nanogram sensitivity to directly quantify the mass uptake of water in the thin Nafion films in real time. The initial dry mass of sample was determined by allowing the film to equilibrate under dry nitrogen until the resonance frequency was stable. Water mass uptake during absorption and desorption was determined by relating changes in the resonance frequency to mass uptake using the Sauerbrey equation.[30]

RESULTS AND DISCUSSION

Structure of Thin Nafion Films. The specular neutron reflectivity data (symbols) and fitting results (lines) for thin Nafion films on both the hydrophobic and hydrophilic OSG surfaces are presented in Figure 1. The films were equilibrated at either 0% RH or 90% RH at 33 °C, a condition which was verified when successive, several-hour-long measurements (not shown here) did not produce observable changes in the data. Qualitatively, all of the reflectivity data exhibit a beating of multiple interferences in the Kiessig fringes, indicating a multilayer structure. In the dry films, the presence of two length scales is explained by the presence of the distinct OSG sublayer and the thin Nafion film itself. We note the emergence of a lower frequency oscillation when comparing the dry to humidified films. This indicates the emergence of new layers upon the hydration of the thin Nafion film. There is a strong contrast in the neutron scattering length density between the

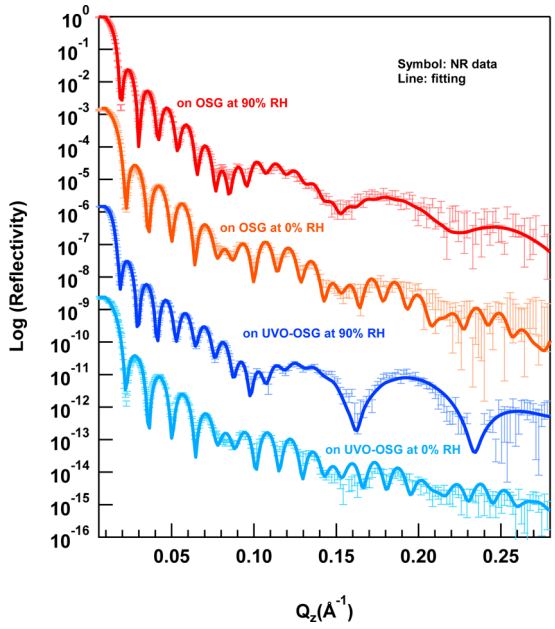

Figure 1. Specular neutron reflectivity data (symbol) and the best model fits (line) for thin Nafion films on OSG-modified substrates: hydrophobic surface (OSG, red) and hydrophilic surface (UVO-OSG, blue). For each sample, the reflectivity data were collected at 90% RH and then 0% RH.

proton-deficient Nafion and the proton-rich water transport domains. Thus, the transport domains become "visible" in neutron scattering and reflectivity measurements under full hydration. The appearance of additional periodicities in the specular reflectivity geometry where the momentum transfer is perpendicular to the film suggests a layering of the water transport domains parallel to the surface. Previously, Dura and co-workers fit in-situ NR measurements of hydrated thin Nafion films on native SiO_2 surface to a model having an interfacial region consisting of lamellar-like water transport channels near the substrate.[21] Here we utilize a similar model to fit the reflectivity data in Figure 1.

The fitting of the NR data in Figure 1 is complicated by the presence of the tunable OSG surface coating on the silicon substrate. The thickness of the OSG layer is comparable to the length scale previously reported for the interfacial layering of the water transport channels. To reduce the uncertainty in the fits, extensive XR and NR measurement were performed on both the hydrophobic and hydrophilic OSG substrates, without the Nafion film, under the same RH conditions used in Figure 1. Fits to the XR and NR data revealed that the OSG films were approximately 8 nm thick on top of a thin native oxide of Si. The OSG films displayed a graded profile where the top half of the film was slightly denser than the bottom half. Here we present only the density profiles from NR fits for both the dry and humidified OSG substrates in Figure 2. Neither of the OSG films displayed any significant signs of swelling upon exposure to humid air, although there was a slight densification as the intrinsic pores of the OSG become condensed with water vapor. The scattering length density profiles for bare OSG films were then "fixed" as the "substrates" when fitting the dry and humidified Nafion film data in Figure 1; only minimal variation within the levels of uncertainty was allowed in the corresponding substrate profiles to reduce the chi squared value for our fits of the Nafion films. This analysis assumes that

dx.doi.org/10.1021/ma400750f | Macromolecules 2013, 46, 5630–5637

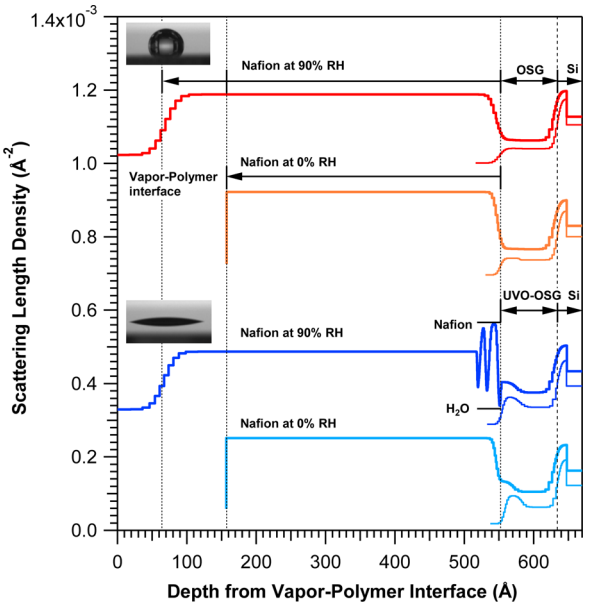

Figure 2. Scattering length density profiles calculated from the best fits to the experimental data in Figure 1 are shown in terms of the SLD as a function of depth from water vapor−polymer interface: The images of water drop in the inset represent hydrophobic OSG surface (red) and hydrophilic UVO-OSG surface. For Nafion film on each surface, the SLD variation at 90% RH is compared to that at 0% RH below. The SLD profile of each OSG layer was independently determined and presented below the profile of corresponding Nafion film for comparison. The SLD profiles are offset for clarity.

the substrates behave in the same way under water vapor whether the OSG film is coated with Nafion or not. To a first approximation this is a reasonable assumption.

After fixing the model parameters for the OSG substrates, we gradually increase the complexity of our model to account for the Nafion film. For the dry films on both the hydrophobic and hydrophilic OSG substrates, the addition of a single Nafion layer having uniform density is sufficient to fit the data with a reduced chi squared value (χ^2) on the order of 2. This is reasonable because under dry conditions there is little scattering length density contrast between the collapsed water transport domains and the fluorinated Nafion matrix. The fits to the NR data are shown in Figure 1, and the corresponding scattering length density profiles are displayed in Figure 2. The fit value for the scattering length density of the homogeneous Nafion layer is consistent with the value for pure Nafion (2.089×10^{-4} Å^{-2}) calculated from the measured density and molecular structure.[21] The fitting routines employed thus far appear to yield reasonable results. A similar approach was employed for fitting the Nafion films under 90% RH. At first the NR data were modeled with the addition of a single uniform layer of Nafion. For the film on the hydrophobic OSG surface, this was sufficient to fit the reflectivity data with χ^2 on the order of 2. The uniform scattering length density through the thickness of the Nafion, even near the OSG interface, suggests a lack of interfacial ordering. However, a single Nafion layer was insufficient to fit the reflectivity data of the humidified film on the hydrophilic substrate. As shown in the Supporting Information (Figure S1), this single layer fit fails to parametrize several characteristics of the reflectivity data and results in χ^2 of approximately 10. Using the previous observations of alternating water-rich and water-deficient domains adjacent to the substrate interface,[21] we sequentially added layers to our model to reduce χ^2 of the fitting. Somewhere between three and five interfacial layers starting with water-rich layer next to the hydrophilic substrate were required to reduce χ^2 of the fit to about 2, consistent with our previous fits. Figure 1 shows the best fit to the data using the five interfacial layer model while Figure 2 shows the corresponding scattering length density profile for the Nafion on the hydrophilic substrate. Away from the interface the scattering length density approaches that of the Nafion layer on the hydrophobic substrate. This indicates that the noninterfacial bulklike Nafion contains similar amounts of water at a given RH, regardless of the substrate. Comparisons with the scattering length densities of the pure water and dry Nafion suggest that the interfacial lamellae are strongly enriched with either water or Nafion, as previously reported.[21,23] This observation is also consistent with previous reports of thin Nafion films at the interface with a wide range of materials[16,17,21−23,31] and suggests that the interfacial layering is controlled by the surface energy of the substrate.

As water molecules infiltrate into the Nafion film and associate with sulfonic acid groups of side chains, water fills and swells the ionic aggregates. We believe these ionic species are selectively attracted by hydroxyl and carboxylic groups of the oxidized (UVO-treated) OSG near the substrate. Since water also has the tendency to wet the UVO-treated OSG surface, enriched water content helps the substrate induce these hydrophilic domains. Because of the continuity of the Nafion chain, this then induces a hydrophilic/hydrophobic layering effect which naturally dissipates with distance from the substrate. The depth profile determined by NR represents the average SLD of a thin film in the perpendicular direction to the surface. Thus, it is impossible to distinguish the in-plane structure of these oriented interfacial transport domains. There are two likely ways in which transport channels might be modeled: either cylindrical water domains in a hydrophobic Teflon-like matrix preferentially lying parallel to the hydrophilic surface (consistent with the cylindrical transport channel model of Schmidt-Rohr[32]) or an interfacial breakdown of the cylindrical domains into lamellar transport channels that run parallel to the substrate. Because the specular NR data are not sensitive to the in-plane structure, we cannot discern between these two extremes. However, it is notable that the composition of water-rich layers vary from nearly 100 vol % H_2O to ≈64 vol % H_2O, suggesting that the interfacial lamellar structure might be more appropriate, as presented by Dura et al.[21]

The NR results on thin Nafion films suggest that the differences in the order and structuring of the ionic domains largely occur only at the substrate interface, but the bulklike Nafion far from the interface is unaffected by the interaction with the substrate. This hypothesis was further investigated by in-situ GISAXS measurements, which has proven to be a useful tool in probing the structure of thin Nafion films.[13,14,23,33] As shown in Figure 3a,b, scattering patterns of thin Nafion films equilibrated at ≈80% RH were taken at an incident angle just above the critical angle of Nafion ($\theta_c \approx 0.12°$) so that the scattering was attributed to the entire film thickness. The scattering for both films clearly show a peak at $q_{max} \approx 0.2$ Å^{-1} ($q = (q_{xy}^2 + q_z^2)^{1/2}$), which is caused by scattering from the ionic, water-containing domains. The scattering intensity as a function of q was obtained from a radial integration of each scattering image and corrected for background scattering and beam intensity fluctuations as represented in Figure 3c.[23,34] The average domain spacing determined from q_{max} was 3.2 ± 0.1 nm

dx.doi.org/10.1021/ma400750f | Macromolecules 2013, 46, 5630−5637

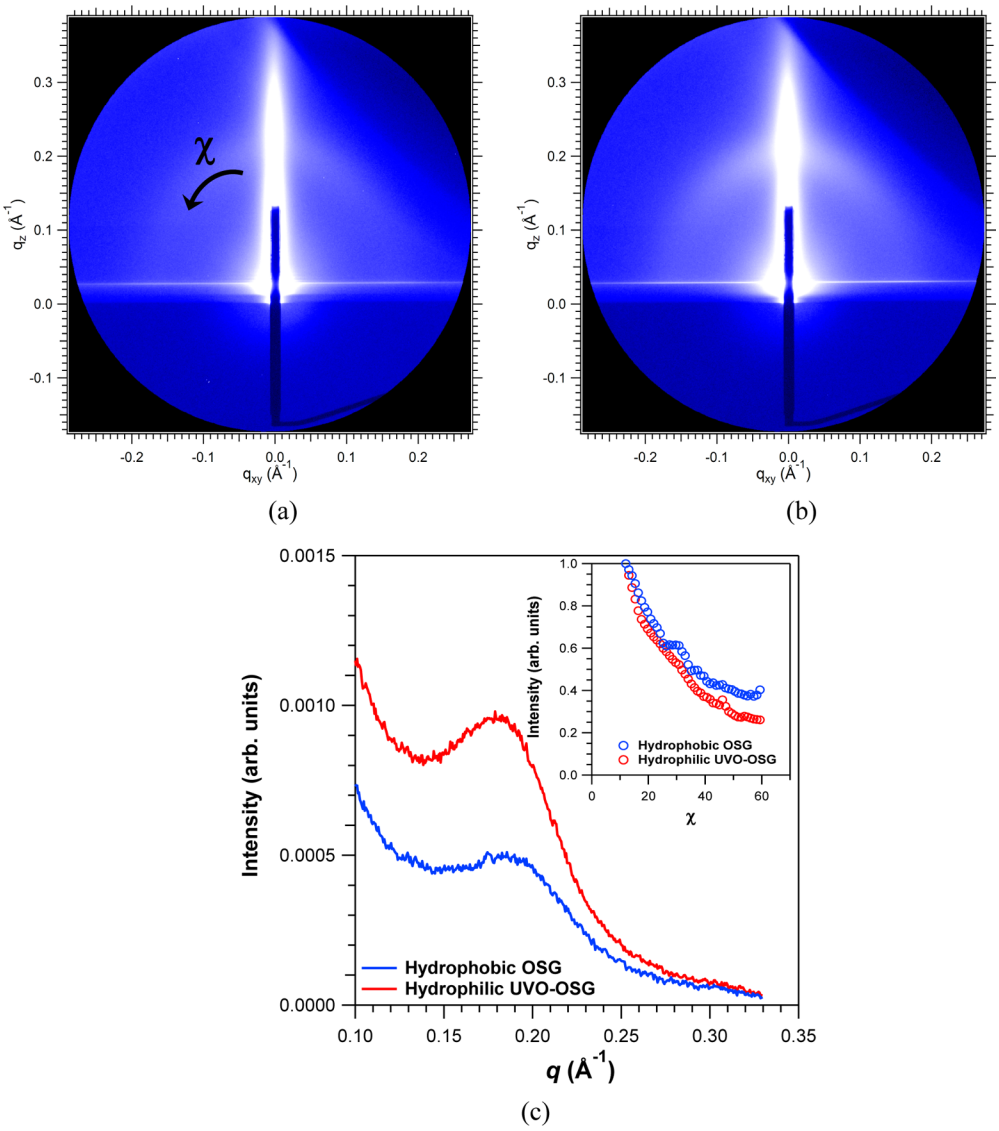

Figure 3. Characteristic GISAXS images taken, in situ, at 80% RH just at an incident angle of above the critical angle ($\theta_c \approx 0.12°$) of thin Nafion films on (a) hydrophobic OSG surface and (b) hydrophilic UVO-OSG surface. (c) Radial integration of each scattering image after background scattering and beam intensity fluctuations are corrected. The inset shows the normalized scattering intensity of the ionomer peak as a function of the azimuthal angle (χ).

and 3.3 ± 0.1 nm for films on the hydrophobic and hydrophilic substrates, respectively. The distance over which the ionic domains are well-correlated was estimated from the peak width and determined to be 15 ± 1 nm for the film on the hydrophobic surface OSG and 16 ± 2 nm for the film on the hydrophilic surface. In Figure 3c, we do see an apparent increase in the overall scattering intensity on the hydrophilic substrate relative to the hydrophobic substrate. However, we caution that these scattering intensities are not on an absolute intensity scale; we cannot comment on the concentration of the scattering domains. We can only conclude that the characteristic length scales of the scattering domains in the two films are comparable within error. The inset of Figure 3c also shows that the normalized scattering intensity at q_{max} decreases significantly as a function of the azimuthal angle (χ). Although both Nafion films show rings of scattering indicating that a portion of the ionic domains are oriented randomly to the substrate, we note an anisotropic distribution of scattering intensity. It results from large population of the domains that are oriented parallel to the substrate. But, the distributions of this anisotropy are comparable regardless of the substrate. Thus, similar azimuthal distributions of the scattering intensity support the idea that the overall structure and orientational order of the ionic domains in the noninterfacial Nafion are consistent for both films on the hydrophobic and hydrophilic substrates and are largely unaffected by the interfacial interactions.

Water Transport of Thin Nafion Films. The major component of Nafion is a highly fluorinated Teflon-like matrix with minor component sulfonic acid-rich water transport domains percolating throughout the hydrophobic matrix.[32,35] The interfacial layering parallel to the hydrophilic substrate would seem to suggest that water transport parallel to the substrate would be easier than that in the perpendicular direction. If the "substrate" were an active catalyst particle or an electrode, this anisotropy of water transport may or may not be a source of interfacial impedance in a functional fuel cell depending on the orientation of water transport domains with respect to the catalytic sites. To answer this question, we

dx.doi.org/10.1021/ma400750f | *Macromolecules* 2013, 46, 5630−5637

explored how the presence of this interfacial layering affects the water transport kinetics in thin Nafion films where the interfacial region accounts for ≈7 vol % of the entire humidified film at 90% RH (as shown in Figure 2). Figure 4 shows a series of QCM mass uptake curves as a function of time for a few cycles between 0% and 70% RH for both the bare (short time) and Nafion coated (long time) substrates, when the substrate is either hydrophobic or hydrophilic. The curves for the hydrophobic and hydrophilic OSG surfaces are shifted in time for clarity. At some arbitrary time point, both curves display a dramatic vertical shift in terms of mass change. This represents the change in mass of the quartz resonator after the Nafion film is spin-cast onto the previously bare substrate. Both before and after this dramatic vertical shift, there are two more subtle cycles of mass uptake that represent cycles between 0% and 70% RH at ambient temperature. Prior to the deposition of Nafion, these changes in mass represent water adsorbing/absorbing onto/into the bare OSG substrates. As one expects, the amount of water adsorption/absorption for the hydrophilic substrate is greater than the hydrophobic substrate (≈5.5 times); water wets the hydrophilic surface preferentially. This is an important baseline as it indicates how big the effect of surface adsorption is in the measurements. We do not believe that water is able condense inside the intrinsic pores of the OSG. The internal surfaces of the pores are intrinsically hydrophobic, and only the top surface of the OSG is rendered hydrophilic by the UV ozone treatment, suggesting that only water adsorption, not absorption, occurs on the OSG layer. This is also consistent with the speed and reversibility of the adsorption/desorption cycles on the bare OSG substrates. After the Nafion has been deposited on the substrates, the changes upon cycling between 0% and 70% RH are more significant, reflecting water adsorption/absorption onto/into the Nafion coated substrates. We cannot rigorously separate between adsorption and absorption effects from the QCM measurements directly, but the results are as expected. The Nafion coated hydrophilic substrate picks up more water (≈1.7 times) than the Nafion coated hydrophobic substrate, generally consistent with a recent report on similar surface energy variation of the substrate.[31] The hydration number, λ, the number of moles of water per mole of sulfonic acid groups, was

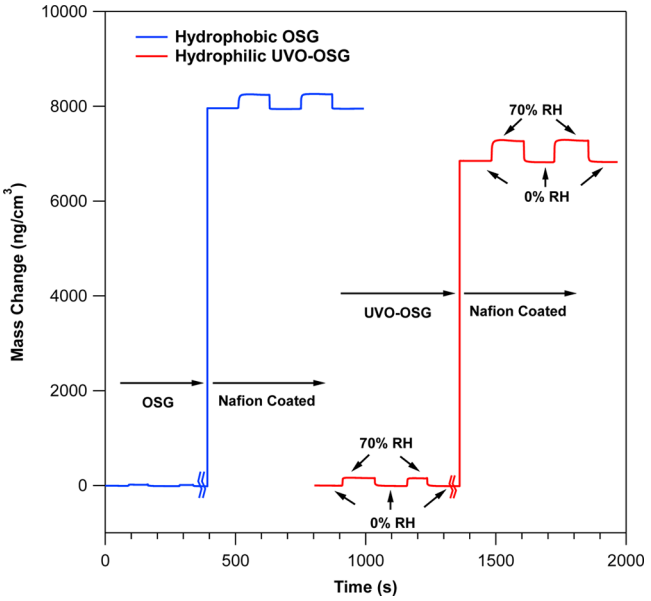

Figure 4. Water sorption behaviors of the bare (short time) and Nafion coated (long time) substrates during the cycles of exposures to 0% RH and 70% RH: Mass changes during water absorption and desorption experiments are combined sequentially before and after Nafion is spin-cast on hydrophobic OSG surface (blue) and hydrophilic UVO-OSG surface (red), as indicated by the brackets. The curves for the hydrophobic and hydrophilic OSG surfaces are shifted in time for clarity. For each surface, the difference between upper baseline and lower baseline represents mass of Nafion deposited on the surface.

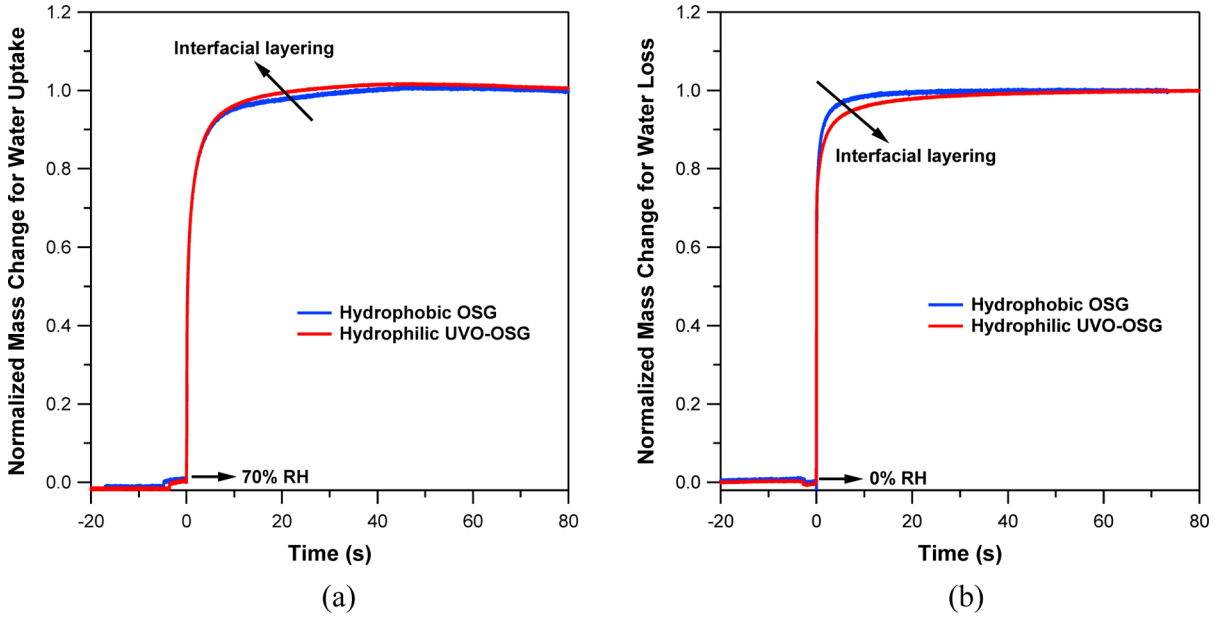

Figure 5. (a) Water absorption at 70% RH and (b) water desorption at 0% RH of Nafion coated substrates: hydrophobic OSG surface (blue, without the interfacial layering) and hydrophilic UVO-OSG surface (red, with the interfacial layering). Mass changes for water uptake and water loss were normalized using $(M_t - M_0)/(M_\infty - M_0)$, where M_t is mass change measured at time t.

dx.doi.org/10.1021/ma400750f | Macromolecules 2013, 46, 5630−5637

calculated to be 2.3 ± 0.2 and 4.0 ± 0.2 for the Nafion coated on the hydrophobic and hydrophilic substrates, respectively. Recall that the NR SLD results indicate that away from the interface the two Nafion films absorb similar amounts of water at a given RH. If the mass uptake measured at 70% RH on the bare hydrophilic substrate is subtracted from the mass change at 70% RH after the deposition of Nafion, then one calculates a λ = 2.5 ± 0.2 for water absorption in the "noninterfacial" regions of the Nafion film, a value comparable with water uptake in the Nafion film on the hydrophobic substrate. The additional water uptake on the hydrophilic substrate is attributed to the water accumulation near the OSG layer, driven by favorable attraction of hydrophilic hydroxyl and carboxylic groups of UVO-treated OSG. Both the NR and the QCM appear to give comparable and consistent estimates on the water uptake in the Nafion films, which may be extended to the interfacial ordering of the water transport domains near the hydrophilic substrate. If the excess water associated with the interface, measured by the QCM, was assumed to have a density of bulk water (1.0 g/cm^3), the resulting thickness would be approximately equal to 1.6 nm for this additional "layer". This estimate is the same order of magnitude with excess water added to the Nafion layer on the hydrophilic OSG in Figure 2 (Supporting Information 2).

Real-time kinetics of water sorption in thin Nafion films were recorded by tracking the fundamental resonance and first overtone frequencies of the quartz crystal as a function of absorption/desorption time. These two resonances gave identical values for the mass change as a function of time. As shown in Figure 5, most of absorption and desorption occurs on short time scales, almost instantaneously. While absolute magnitudes of the mass changes are different on the different substrates, as discussed above, the time dependence of the mass changes that are normalized to the mass at equilibrium are almost identical for both water uptake and water loss. With and without the interfacial layering, the effective transport kinetics do not show any noticeable differences for normalized mass changes up to 0.94 ± 0.03 on absorption or 0.82 ± 0.03 on desorption; the two curves lie right on top of each other. Only slight differences are observed at longer times during the final normalized mass gain of 0.06 on absorption and mass loss of 0.18 on desorption. These subtle differences happen over time scales of several tens of seconds, which is an order of magnitude lag compared to the overall change in the film. To a first approximation, the interfacial layering of the transport domains near the interface appears to have little effect on the transport kinetics, despite the fact that they are oriented orthogonal to the primary direction of transport.

We suspect that the differences in the late stage sorption reflect the propensity for water to reside near the buried interface.[36] The hydrophilic nature of the substrate increases the thermodynamic driving force for water to diffuse and accumulate near the interface. Consequently, we observe that water uptake occurs faster on the hydrophilic substrate. One could also argue this is not just a thermodynamic effect, but also a polymer dynamic one where the excess water helps plasticize the Nafion; the transport kinetics are known to increase with the hydration level. However, measurements on desorption seem to favor the thermodynamic argument. The hydrophilic substrate dehydrates more slowly at the longer time scales, suggesting that the favorable interaction between the water and the substrate helps retain water. If the underlying cause was purely due to polymer dynamics, one might expect the higher interfacial hydration number to lead to faster desorption on the hydrophilic substrate. This is not observed. It indicates that the ordering of the transport domains near the interface is strongly correlated with the excess water being there. When the thin Nafion film is exposed to water vapor, the process occurs sequentially through vapor adsorption at the film surface followed by swelling and diffusion of the water perpendicularly into the film;[18,34] the absorbed water reaches the buried interface last. This is probably why the transport kinetics through the majority of the film in the initial stages are, to a first approximation, not affected by substrate surface energy; the ordered channels have not yet had time to form. Generally, the desorption process is faster than the absorption process because polymer deswelling and relaxation is not necessary for water to escape from Nafion film.[37] Without restructuring or collapse of the oriented interfacial transport domains, water desorption kinetics is more affected by the interfacial region, and thus the larger difference occurs in the later sorption response during the larger normalized mass loss of 0.18. However, it would be difficult to separate a characteristic time scale for polymer motion dictating the kinetics of interfacial ordering from the time scale for moisture transport. We note the small volume fraction (≈7%) of the interfacial layering region. Preliminarily, we observe that the fraction of interfacial region increases as the film thickness decreases. Then, we would expect that increased correlation of two time scales in thinner film will result in larger effect of the interfacial layering on the transport kinetics.

In closing, we point out that no significant changes are observed in the relative transport kinetics of water into and out of Nafion films of similar thickness on the substrates of different wetting characteristics, despite the fact that these two systems exhibit different interfacial morphologies. Our earlier investigation of Nafion thin films on SiO_2,[23] where interfacial lamellae have been shown to exist,[21] found the transport kinetics of water to depend on film thickness below approximately 60 nm. It was speculated that in this thickness regime the interfacial layering of the transport domains comprised a significant volume fraction of the film and was a possible origin for the observed reduction in the effective diffusion coefficient of water in the thin films since the transport channels would be oriented perpendicular to the primary direction of transport. The results presented here show that retardation in the transport kinetics in thin films is not due to the interfacial morphology of the transport domains but rather a general effect of confinement. Moreover, the findings presented here provide guidance to improve the level of detail in the modeling of the transport of water in PEFCs, especially within the composite electrode layer. Specifically our results show that surface wettability of the substrate can influence the total amount of water in the system but that the transport kinetics across the thin ionomer film are largely unaffected, both of which are important factors with regard to water management in a working PEFC.

■ CONCLUSIONS

Here we have investigated how the hydrophilicity of the supporting substrate influences the interfacial nanostructure of thin Nafion film confined at a thickness relevant to the MEA and if corresponding water transport kinetics is affected by the interfacial nanostructure. Neutron reflectivity and quartz crystal microbalance measurements provide strong evidence that the favorable interactions of a hydrophilic organosilicate surface with sulfonate groups in Nafion lead to interfacial ordering of

the water transport domains parallel to the interface as well as an enhanced water uptake relative to a hydrophobic organosilicate surface. The nature of the interaction between Nafion and the substrate is dependent on the surface energy. The increased water uptake throughout the film, but enhanced in the interfacial layering region, quantified by neutron reflectivity is similar to the estimation of excess water content by quartz crystal microbalance. In-situ quartz crystal microbalance measurements show that the kinetics of absorption and desorption are not affected by the interfacial ordering of the transport domains for initial mass changes up to 82−94% of the total changes, but the kinetics of the final 6−18 mass % are different. Thin Nafion films on hydrophilic substrates tend to hydrate slightly faster than their hydrophobic counterparts and correspondingly hold onto their absorbed moisture slightly longer upon desorption.

■ ASSOCIATED CONTENT

Ⓢ Supporting Information

Comparison of the best model fits with and without interfacial layering of water transport domains. This material is available free of charge via the Internet at http://pubs.acs.org.

■ AUTHOR INFORMATION

Corresponding Author

*E-mail: sangcheol.kim@nist.gov (S.K.); kirt.page@nist.gov (K.A.P.).

Notes

The authors declare no competing financial interest.

■ ACKNOWLEDGMENTS

The authors thank Prof. R. M. Laine (University of Michigan and Mayaterials Inc.) for providing the OSG precursors, Dr. H. W. Ro for helping sample preparation, and Dr. W. L. Wu for helpful discussions on reflectivity data analyses. Research was carried out in part at the Center for Functional Nanomaterials and the National Synchrotron Light Source, Brookhaven National Laboratory, which is supported by the U.S. Department of Energy, Office of Basic Energy Sciences, under Contract DE-AC02-98CH10886.

■ REFERENCES

(1) Certain commercial equipment, instruments, or materials are identified in this paper in order to specify the experimental procedure adequately. Such identification is not intended to imply recommendation or endorsement by the National Institute of Standards and Technology, nor is it intended to imply that the materials or equipment identified are necessarily the best available for the purpose.

(2) Ticianelli, E. A.; Derouin, C. R.; Redondo, A.; Srinivasan, S. *J. Electrochem. Soc.* **1988**, *135*, 2209.

(3) Paik, W.; Springer, T. E.; Srinivasan, S. *J. Electrochem. Soc.* **1989**, *136*, 644.

(4) Litster, S.; McLean, G. *J. Power Sources* **2004**, *130*, 61.

(5) More, K. L. *DOE Hydrogen Program Annual Progress Report*, Nov 2005.

(6) Mashio, T.; Malek, K.; Eikerling, M.; Ohma, A.; Kanesaka, H.; Shinohara, K. *J. Phys. Chem. C* **2010**, *114*, 13739.

(7) Xie, J.; Garzon, F.; Zawodzinski, T.; Smith, W. *J. Electrochem. Soc.* **2004**, *151*, A1084.

(8) Berg, P.; Novruzi, A.; Volkov, O. *J. Fuel Cell Sci. Technol.* **2008**, *5*, 021007.

(9) Kim, Y. H.; Oblas, D.; Angelopoulos, A. P.; Fossey, S. A.; Matienzo, L. J. *Macromolecules* **2001**, *34*, 7489.

(10) Weber, A. Z.; Newman, J. *J. Electrochem. Soc.* **2003**, *150*, A1008.

(11) Majsztrik, P.; Bocarsly, A.; Benziger, J. *J. Phys. Chem. B* **2008**, *112*, 16280.

(12) Goswami, S.; Klaus, S.; Benziger, J. *Langmuir* **2008**, *24*, 8627.

(13) Bass, M.; Berman, A.; Singh, A.; Konovalov, O.; Freger, V. *J. Phys. Chem. B* **2010**, *114*, 3784.

(14) Bass, M.; Berman, A.; Singh, A.; Konovalov, O.; Freger, V. *Macromolecules* **2011**, *44*, 2893.

(15) Zhao, Q. A.; Majsztrik, P.; Benziger, J. *J. Phys. Chem. B* **2011**, *115*, 2717.

(16) Liu, J. W.; Selvan, M. E.; Cui, S.; Edwards, B. J.; Keffer, D. J.; Steele, W. V. *J. Phys. Chem. C* **2008**, *112*, 1985.

(17) Selvan, M. E.; Liu, J.; Keffer, D. J.; Cui, S.; Edwards, B. J.; Steele, W. V. *J. Phys. Chem. C* **2008**, *112*, 1975.

(18) Kendrick, I.; Kumari, D.; Yakaboski, A.; Dimakis, N.; Smotkin, E. S. *J. Am. Chem. Soc.* **2010**, *132*, 17611.

(19) Kunimatsu, K.; Yoda, T.; Tryk, D. A.; Uchida, H.; Watanabe, M. *Phys. Chem. Chem. Phys.* **2010**, *12*, 621.

(20) Kongkanand, A. *J. Phys. Chem. C* **2011**, *115*, 11318.

(21) Dura, J. A.; Murthi, V. S.; Hartman, M.; Satija, S. K.; Majkrzak, C. F. *Macromolecules* **2009**, *42*, 4769.

(22) Murthi, V. S.; Dura, J. A.; Satija, S.; Majkrzak, C. F. *ECS Trans.* **2008**, *16*, 1471.

(23) Eastman, S. A.; Kim, S.; Page, K. A.; Rowe, B. W.; Kang, S. H.; DeCaluwe, S. C.; Dura, J. A.; Soles, C. L.; Yager, K. G. *Macromolecules* **2012**, *45*, 7920.

(24) Lee, H. J.; Soles, C. L.; Lin, E. K.; Wu, W. L.; Liu, Y. *Appl. Phys. Lett.* **2007**, *91*, 172908.

(25) Ro, H. W.; Popova, V.; Chen, L.; Forster, A. M.; Ding, Y. F.; Alvine, K. J.; Krug, D. J.; Laine, R. M.; Soles, C. L. *Adv. Mater.* **2011**, *23*, 414.

(26) Wu, W. L.; Wallace, W. E.; Lin, E. K.; Lynn, G. W.; Glinka, C. J.; Ryan, E. T.; Ho, H. M. *J. Appl. Phys.* **2000**, *87*, 1193.

(27) Vogt, B. D.; Pai, R. A.; Lee, H. J.; Hedden, R. C.; Soles, C. L.; Wu, W. L.; Lin, E. K.; Bauer, B. J.; Watkins, J. J. *Chem. Mater.* **2005**, *17*, 1398.

(28) Dura, J. A.; Pierce, D. J.; Majkrzak, C. F.; Maliszewskyj, N. C.; McGillivray, D. J.; Losche, M.; O'Donovan, K. V.; Mihailescu, M.; Perez-Salas, U.; Worcester, D. L.; White, S. H. *Rev. Sci. Instrum.* **2006**, *77*, 074301.

(29) Kienzle, P. A.; O'Donovan, K. V.; Ankner, J. F.; Berk, N. F.; Majkrzak, C. F. http://www.ncnr.nist.gov/reflpak, 2000−2006.

(30) Sauerbrey, G. *Z. Phys.* **1959**, *155*, 206.

(31) Wood, D. L.; Chlistunoff, J.; Majewski, J.; Borup, R. L. *J. Am. Chem. Soc.* **2009**, *131*, 18096.

(32) Schmidt-Rohr, K.; Chen, Q. *Nat. Mater.* **2008**, *7*, 75.

(33) Modestino, M. A.; Kusoglu, A.; Hexemer, A.; Weber, A. Z.; Segalman, R. A. *Macromolecules* **2012**, *45*, 4681.

(34) Smilgies, D. M. *J. Appl. Crystallogr.* **2009**, *42*, 1030.

(35) Gebel, G. *Polymer* **2000**, *41*, 5829.

(36) Wu, W. L.; Orts, W. J.; Majkrzak, C. J.; Hunston, D. L. *Polym. Eng. Sci.* **1995**, *35*, 1000.

(37) Satterfield, M. B.; Benziger, J. B. *J. Phys. Chem. B* **2008**, *112*, 3693.